Preparation and Characterisation of Nanostructured Metal Films

Samuel Moore
Supervisors: W/Prof Jim Williams, Prof Sergey Samarin
Honours Thesis submitted as part of the B.Sc. (Honours) degree
in the School of Physics, University of Western Australia

Date of submission: 02/11/2012

Declaration

I declare that this thesis contains less than 40 pages, excluding: the title page, this declaration, acknowledgements, the table of contents, and references.

Acknowledgments

I am extremely grateful for the support offered to me by many individuals during this project. There aren't many synonyms for "Thanks", so I'm afraid this section may be a little repetitive.

Thanks to my supervisors Prof Sergey Samarin and W/Prof Jim Williams for envisioning the project, and their invaluable support throughout the year. I would also like to thank staff members at CAMSP for assisting with the supervision of this project. In particular I am extremely grateful for the help and advice given by Dr Paul Gualiardo during the construction and testing of the Total Current Spectroscopy experiment.

Thanks to CMCA for producing the SEM images which proved a invaluable aid for discussing the structure of the metallic-black films. Thanks to Jeremy Hughes for lending me some samples for ellipsometric analysis (even though I did not get around to studying those samples). I would also like to endorse the team at J.A Woolam, who provided replacement pins for the ellipsometer alignment detector at no charge after one of the original pins became mysteriously damaged.

Congratulations to Jeremy Hughes who successfully predicted that the emission current of the electron gun was varying periodically less than a quarter of the way through the first period. Condolences to Alexander Mazur, whose theory that the vacuum chamber contained a pulsar proved unfounded.

Thanks to all my family and friends for their support and for continuing to put up with my slow descent into madness during the last 12 months.

Finally, perhaps as a result of the aforementioned madness, I would also like to thank the various pieces of equipment and inanimate objects which have been crucial to the success of this project. This includes the ellipsometer, the ADC/DAC box, my laptop computer "Cerberus", and the two electrometers that I relied upon so heavily. Rest in peace Keithly 610B. Your death was not in vain.

Abstract

Preparation and Characterisation of Nanostructured metal films

Keywords: plasmonics, thin films, silver, gold, nanostructures, optical transmission spectroscopy, ellipsometry, total current secondary electron spectroscopy, scanning electron microscopy

Black metal films have been used for a wide range of optical applications for many decades due to their unusual absorbsion properties [1] [2]. Black metal films have recently been shown to increase the efficiency of thin film solar cells [3].

In this project we have produced a range of silver and gold nanostructured films for study using optical and electronic spectroscopic techniques. Scanning electron microscopy images have been used to study the structural differences between black and non-black metal films. A Total Current Spectroscopy experiment has been designed and integrated with sample preparation technology; this allowed us to perform analysis of surfaces in situ. Optical transmission spectroscopy has been used to compare the transmissive behaviour of black and non-black films under visible wavelengths. Variable Angle Spectroscopic Ellipsometry (VASE) has been employed for detailed measurements and modelling of samples.

SEM images confirm that the structure of black metal films is extremely complicated when compared to a non-black film. With Total Current Spectroscopy, we have demonstrated a change in surface potential when a Black Ag film was deposited onto an existing Ag film. Ellipsometric modelling for very thin Ag and Black Ag films shows a notable difference in optical constants of the two films.

Contents

Chapter 1

Introduction

Interest in the optical properties of nanostructured thin films can be traced back to the 19th century. In the 1857 Bakerian Lecture, Michael Faraday discussed a range of unusual optical effects exhibited by thin films of Au and other metals subjected to different treatements [4]. The role of metallic nanoparticles of gold in producing the colours of stained glass was first investigated by Garnet in 1904 [5] using Rayleigh's theory for scattering of light from spherical particles. A few years later, Gustav Mie developed a more complete theory of light scattering for spherical nanoparticles; Mie's theory is still widely used accross many disciplines [6] [7].

Many of the properties investigated by Faraday are now understood in terms of the behaviour of the electron gas in a metal, and in particular the ability for thin metal films to support plasmonic resonance effects. A plasmon is a quasiparticle which describes the collective oscillation of conduction electrons in a metal. The behvaiour of plasmons is well understood in terms of classical models for a free electron gas; in the Lorentz model electrons are treated as damped harmonic oscillators. When light is incident on a metal, the electrons may collectively resonate in response to the sinusoidal forcing field.

Recently there has been much interest in the exploitation of plasmonic effects in nanoscale devices for a bewildering array of applications from improvement of photovoltaic solar cell efficiency [8, 9] to biosensing [10], and even the potential for plasmonic based computing devices [11].

A fascinating phenomena first observed in the 1930s [1] is the tendency for metal films deposited in high pressure[1] atmospheres to appear completely black at visible

[1] Of the order of 10^{-2}mbar

wavelengths. Such films have found use in a range of optical applications as near perfect black bodies with very low thermal mass [1, 12, 2, 13].

Recently, so called "black metal" films have been found to enhance the efficiency of thin film solar cells; this is consistent with the presence of plasmonic effects in the films [3].

The aim of this project has been the preparation and characterisation of thin metal film samples, with a focus on black metal films. We have also investigated the possibility for plasmonic behaviour in Black metal films. We have prepared samples for subsequent study with both electronic and optical spectroscopic techniques.

The remainder of this report will be organised as follows: in chapter 2 we will present an overview of past research into the characterisation of black metal films, followed by a brief explanation of plasmonic behaviour based on the Lorentz model. Chapter 3 will give an overview of the two main experimental techniques employed during this study (Total Current Spectroscopy and Ellipsometry). In chapter 4 we will present results and discussion of experiments, which will be followed with the conclusions of this study.

A Note on Terminology

There is some possibility for confusion when referring to metal films evaporated at high pressure, which appear black at visible wavelengths, and metal films evaporated at low pressure, which are typically highly reflective. In the remainder of this report, we will refer to the former as "black metal" films and the latter simply as "metal" films (regardless of whether the film is thick enough for the colour to be visible to the naked eye).

Chapter 2

Overview

2.1 Black Metal Films

So called black metal films[1] are the result of deposition of metal elements at a relatively high pressure[2] or "bad vacuum". The films are named due to their high absorbance at visible wavelengths; a sufficiently thick film will appear black to the naked eye. There is a remarkable contrast between such films and metal films deposited under low pressure[3], which are typically highly reflective and brightly coloured at comparable thicknesses. It has been established that Black metal films may be prepared in any gas, but when oxygen is present the resulting films contain tungsten oxides due to the use of tungsten heating filaments for the deposition of films[2] [14].

The formation of black-metal films at high pressure has been known since the early 20th century, with the first papers on the subject published by Pfund in the 1930s, motivated by the potential application of black-metal films to radiometetric devices [1], [15]. Pfund established the conditions for formation of black-metals and showed that the transmission spectrum of metallic black films is almost zero in visible wavelengths, but increases to a plateau in the far infrared. Subsequent researchers have also focused on measuring the properties of black-metal films as a function of preparation conditions, with the aim of producing selective filters for infra-red detectors. [12] [2]. More recently, it was shown that black-Au coatings can be used to increase the efficiency of thin film solar cells [3].

[1] Naming conventions vary in the literature
[2] of the order of 10^{-2} mbar
[3] less than 10^{-5}mbar

There have been several attempts to relate the structure of black-metal films to measured optical and electrical properties. Metallic nanostructured films deposited at low pressures generally consist of a series of metallic islets; for such films, Mie theories of scattering are often used. However, it is clear that black-metal films usually consist of a highly irregular strandlike structure; Mie theories fail to accurately predict the optical properties of such films [14].

Harris et al. have produced experimental results of the transmission of black-metal films from visible wavelengths to the far-infrared. By modelling black-metal films as consisting of layers of "yarn like" metal strands, Harris et al. have arrived at an expression for the electron relaxation time of Au-black, leading to a calculated transmission spectrum in good agreement with experimental results [13].

The optical properties of black-metal films have been found to vary due to changes in structure when the film is exposed to atmosphere, or is heated [16]. This "degradation" of the black-metal films is inconvenient for maintaining consistent calibration of devices. Recently there has been interest in artificial "blackening" of metal surfaces for optical applications. These "meta-materials" offer a promising alternative to the traditional black-metal films, due to the ability to more precisely control properties of the film. In particular, artifially blackened metal films have been produced which suppress reflection of light via surface plasmon resonances [17].

In light of the wealth of previous research, the aims of this project were first to reproduce black-metal films using equipment available in the CAMSP research group, and then employ several techniques for the study of these samples in comparison with other metal films. Most of the existing research has been conducted using optical transmission or reflection spectroscopy techniques. A total current secondary electron spectroscopy experiment was therefore integrated into the sample preparation vacuum chamber, to allow for almost immediate study of prepared samples using this technique. A Variable Angle Spectroscopic Ellipsometer (VASE) has been used in an attempt to relate the optical and structural properties of the samples. We have also used optical transmission spectroscopy at visible wavelengths to characterise the transmission of black-metal films.

2.2 Plasmonics

Since optical properties of nanostructured films are often determined by plasmon-photon interaction, a brief description will be given of plasmonic behaviour in such films. Generally the optical properties of a metal are modelled using a combination of classical and quantum theories. For noble metals (eg: Au and Ag), conduction band electrons are well described by free electron gas models [18].

2.2.1 Bulk Plasmons

In the Lorentz model, electrons responding to incident light are modelled as non-interacting, damped and forced harmonic oscillators. For each electron:

$$m\frac{d^2\boldsymbol{x}}{dt^2} = -m_e\Gamma\frac{d\boldsymbol{x}}{dt} - m_e\omega_0^2\boldsymbol{x} - e\boldsymbol{E_0}e^{-i\omega t} \tag{2.1}$$

where m is the electron mass, $\boldsymbol{x}$ is the displacement of the electron from equilibrium, Γ is the damping constant, $-m\omega_0^2\boldsymbol{x}$ is the restoring force, and $-e\boldsymbol{E_0}e^{-i\omega t}$ is the forcing term due to an incident plane wave of frequency ω.

The polarisation density $\boldsymbol{P}$[4] of the electron gas describes the material's response to the incident light. It can be writen as [18]:

$$\boldsymbol{P} = \tilde{\epsilon}\boldsymbol{E} = -eN\boldsymbol{x}(t)$$

Where $\tilde{\epsilon}$ is the psuedo-dielectric constant and N is the number of electrons per unit volume.

Solving for $\boldsymbol{x}(t)$ gives the Lorentz Oscillator expression:

$$\tilde{\epsilon}(\omega) = 1 + \frac{e^2N}{\epsilon_0 m}\frac{1}{\omega_0^2 - \omega^2 - i\Gamma\omega}$$

In the noble metals (Au, Ag, etc), conduction electrons are extremely loosely bound. The Drude model, which neglects the restoring force, is a good model for electron behaviour in these metals. In this case, $\omega_0 = 0$, and:

$$\tilde{\epsilon}(\omega) = 1 - \frac{\omega_p^2}{\omega^2 + \Gamma^2} + i\frac{\omega_p^2\Gamma}{\omega(\omega^2 + \Gamma^2)}$$

[4]Not to be confused with the polarisation state of light

where the Drude Plasma frequency ω_p is:

$$\omega_p = \sqrt{\frac{e^2 N}{\epsilon_0 m}}$$

If Γ is small, (as for the noble metals), then as ω approaches ω_p, the real part of $\tilde{\epsilon}$ approaches zero, and longitudinal oscillating waves may propagate through the material [18]. These oscillations are called "Bulk" or "Volume" plasmons. They were first excited in Electron Energy Loss Spectroscopy (EELS) experiments by Ferrel in 1958 [19].

In real metals, interband transitions contribute to $\tilde{\epsilon}$. The "screened" plasmon frequency is given by:

$$\omega_{sp}^2 = \frac{\omega_p^2}{\epsilon_\infty} - \Gamma^2 \tag{2.2}$$

where ϵ_∞ is a constant representing the real part of $\tilde{\epsilon}$ with the contribution of interband transitions. The accuracy of this formula decreases as $\hbar\omega$ approaches the energy for interband transitions. [18].

From (2.2), it can be seen that interband transitions effectively reduce the frequency at which bulk plasmons are excited. For example, in Ag $\epsilon_\infty \approx 4$ and $\hbar\omega_{sp} = 2.8$ eV. Observed values for the bulk plasmon frequency in Ag are typically $\hbar\omega = 3.8$ eV [20]. Ag's relatively low plasmon threshold energy makes it a material of choice for plasmonic meta-material applications [18].

2.2.2 Surface Plasmons

One of the most important developments leading to the modern field of plasmonics has been the prediction of so called Surface Plasmons (SP) in 1957 by Ritchie [21]. In his paper, Ritchie predicted surface plasmons as the mechanism for energy loss of electrons passing through a thin film, building on previous work by Pines and Bohm [22] [23] [24]. Ritchie's prediction was experimentally verified here at UWA by Cedric Powel and John Swan just three years later [25].

A coupled Surface Plasmon and Photon are referred to as a Surface Plasmon Polariton (SPP). The behaviour of SPPs can be derived by solving Maxwell's equations for p (parallel to the plane of incidence) and s (parallel to the surface) polarised light at the interface between a metal and a dielectric [26].

The Surface plasmon frequency is given by:

$$\omega_s = \frac{\omega_p}{\sqrt{1+\epsilon_a}}$$

where ϵ_a is the dielectric constant for the dielectric. For air, $\epsilon_a = 1$ and $\omega_s = \frac{\omega_p}{\sqrt{2}}$

Theoretically, SPPs can only couple to p polarised light. This makes Ellipsometry, which measures the change in polarisation of reflected light, a useful technique for detecting excitation of SPPs [18].

In order to excite an SPP in a flat surface, some form of "third body" is required to match the wavevector of the photon with the plasmon. The Kretchsman configuration is one possible method, in which light is totally internally reflected at the interface between a glass prism and one side of the metal film. The evanescent fields created at the interface between a thin film and the glass may lead to the excitation of a SPP on the other side of the thin film.

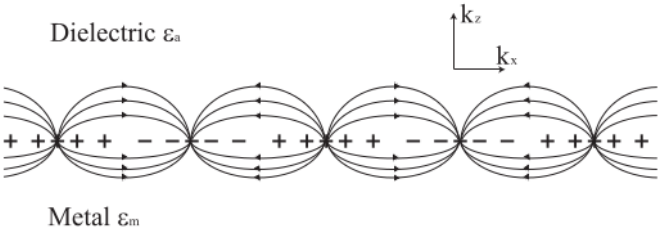

Figure 2.1: Illustration of the charge distribution and electric fields of a surface plasmon polariton taken from Oates et al. [18]

2.2.3 Surface Plasmon Resonances

Due to different boundary conditions, a nanostructured surface exhibits very different plasmonic effects to a smooth surface. Although the term "plasmon" was not coined until the 1950s, Mie's solution for scattering of light from spherical nanoparticles does incorporate the Drude model, and predicts resonance of the free electron gas inside the metal spheres. These are now refered to as Mie plasmons, or surface plasmon resonances (SPR) [26, 18]. The frequency of these resonances is:

$$\omega_{pp}^2 = \frac{\omega_p^2}{\epsilon_\infty + 2\epsilon_a} - \Gamma^2 \tag{2.3}$$

For a pure Drude metal, this reduces to $\omega_{pp} = \frac{\omega_p}{\sqrt{3}}$. Light of frequency ω_{pp} is preferentially scattered.

Chapter 3

Techniques

3.1 Total Current Spectroscopy

The optical properties of metals depend upon both conduction and valance band electrons. At the surface of a material, the electron spectrum (energy levels, band structure and densities of states) may differ greatly from the bulk. This is largely due to the sharp change in potential at the interface; rearrangement of lattice sites, "dangling" molecular bonds, and adsorbed defects are also contributing factors

Total Current Spectroscopy is an electronic spectroscopy technique which is extremely sensitive to the electronic properties of the surface region. The experimental setup for Total Current Spectroscopy can be easily integrated into existing apparatus for sample preparation, which allows for measurements to be made in situ.

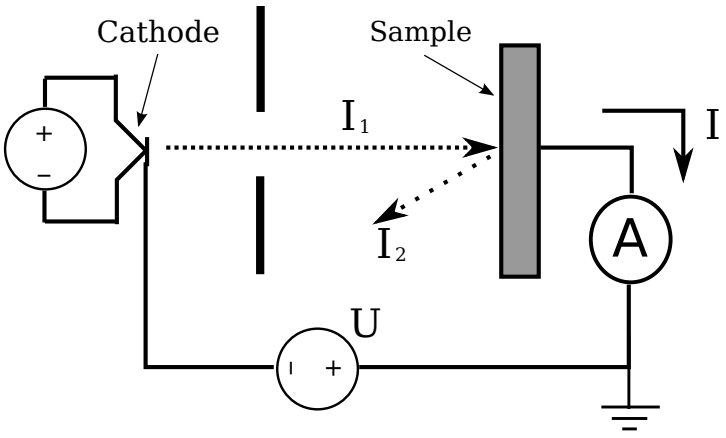

Figure 3.1: A simplified schematic of a Total Current Spectroscopy Experiment

In Total Current Spectroscopy experiments (Figure 3.1), a current of primary

electrons I_1 is directed at a target surface. Upon interacting with the surface, the primary electron beam is split into two components; the transmitted current I, and the secondary electron current I_2. I_2 includes components formed from elastically and inelastically scattered primary electrons, as well as any "true secondary" electrons emitted by the surface.

For each mechanism behind the origin of an electron in I_2, there is an associated "threshold" primary electron energy which must be exceeded before the process can occur. As a result, measurement of changes in I_2 as a function of primary electron energy E_1 provides a sensitive means to characterise properties of the sample under bombardment. The energy E_1 of primary electrons is controlled by adjustment of the potential U applied between the sample and cathode.

Primary electrons are thermionically emitted at a cathode with a distribution in energies. A series of electrodes (an electron gun) focuses the emitted electrons into a beam and produces the current I_1 at the target. A feedthrough connected to the sample holder allows the transmitted current I to be measured external to the vacuum chamber using an electrometer. Measurement of I instead of I_2 is generally preferred, since changes in I can be directly related to changes in I_2.

The total current spectrum (TCS) is defined as:

$$S(E_1) = \frac{dI}{dE_1} = -\frac{dI_2}{dE_1}$$

This result assumes that the primary electron current I_1 is constant. This assumption is generally valid over long time scales once the cathode has reached thermal equilibrium. [1]

3.1.1 General form of $S(E_1)$

In the following, a generalised formula for $S(E_1)$ will be presented as derived by Komolov [27].

The current of primary electrons incident perpendicular to the surface can be

[1] In the final experimental setup, the primary electron current was found to vary by about 2% over the course of several days; far longer than the time taken for total current spectrum measurements (30s to 10min)

written as:

$$I_1(E_1) = eA \int_0^\infty f(E - E_1) dE$$

where $f(E - E_1)$ gives the distribution for electrons of energy E arriving at the surface. $f(0)$ (ie: $E = E_1$) is the maximum of f.

The total secondary current may be written as:

$$I_2(E_1) = eA \int_0^\infty f(E - E_1)\sigma(E) dE$$

Where the cross section $\sigma(E)$ is the probability for a primary electron of energy E to give rise to a secondary electron (of any energy $E_2 \leq E$).

Using $I = I_1 - I_2$, it is straight forward to arrive at a general expression for $S(E_1)$:

$$S(E_1) = eA \left\{ [1 - \sigma(0)] f(-E_1) + \int_0^\infty f(E - E_1) \frac{d\sigma(E_1)}{dE_1} dE \right\} \tag{3.1}$$

All E_1 dependence in the first term is due soley to the primary electron energy distribution. This term is responsible for the first peak in an $S(E_1)$ curve.

The second term contains dependence upon $\frac{d\sigma(E_1)}{dE_1}$. As E_1 is increased past the threshold for a particular interaction, $\sigma(E_1)$ will undergo a sharp change. This corresponds to a narrow maxima or minima in the derivative $\frac{d\sigma(E_1)}{dE_1}$. A corresponding maxima or minima will appear in $S(E_1)$, centred about the threshold for the interaction. The convolution with the primary electron distribution $f(E - E_1)$ has the effect of broadening and lowering these peaks; in other words, the resolution of total current spectroscopy is limited by the distribution of primary electron energies.

The (unphysical) case of a mono-energetic beam is equivelant to setting $f(E - E_1) = \delta(E - E_1)$. In this case, the integrals in the expressions for I and I_2 collapse, and the resulting total current spectrum is:

$$S(E_1) = \frac{dI}{dE_1} = eA \frac{d}{dE_1} (1 - \sigma(E_1)) = eA \frac{d\sigma(E_1)}{dE_1} \tag{3.2}$$

A form of (3.2) is usually assumed when constructing a more detailed theory of secondary electron current formation, as the location of peaks due to $\frac{d\sigma(E_1)}{dE_1}$ is

the same in both (3.2) and (3.1). Figure 3.2 illustrates an idealised total current spectrum.

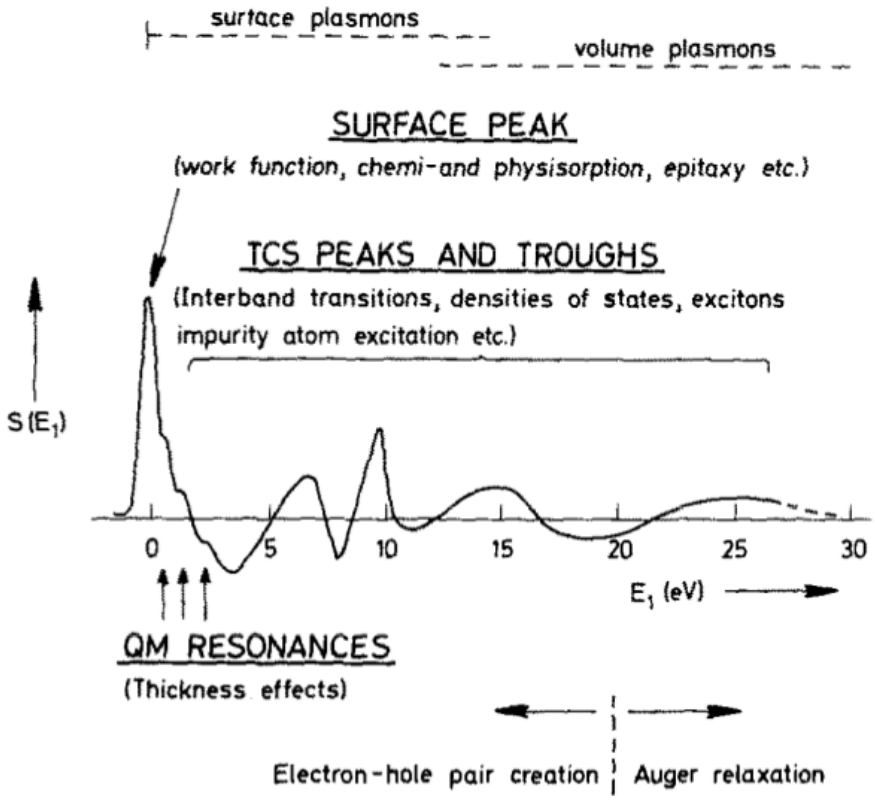

Figure 3.2: An idealised total current spectrum (Komolov et al 1979 [28])

3.1.2 Contact Potential and the Surface Peak

The case $E_1 = 0$ does not in general correspond to $U = 0$. Figure 3.3 describes a simplified step potential model for the surfaces of the cathode and sample. In a classical approximation, primary electrons will be elastically scattered from the sample unless they have energy greater than its vacuum level.

At the cathode, electrons are thermionically excited from the conduction band to the vacuum level. The vacuum levels of the cathode and surface are not generally equal. The contact potential is the difference in work functions of the materials. As U approaches the contact potential, primary electrons are able to penetrate into the sample, and a sharp peak termed the surface peak is seen in $S(U)$. The maxima of this peak occurs at an applied potential U such that $E_1 = 0$; its shape is indicative of $f(E - E_1)$.

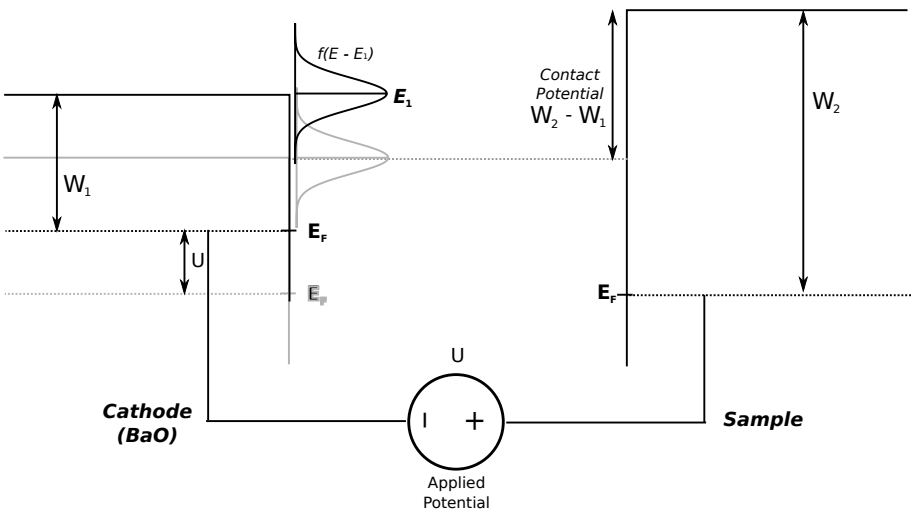

Figure 3.3: Illustration of the step potential model for the surfaces

3.1.3 Electron-Electron Interactions

In the Sommerfield free electron gas approximation, electrons are assumed to be contained within a rectangular potential well, with energies given by $E_k = \frac{\hbar^2 k^2}{2m}$, where $\boldsymbol{k}$ is the electron wave vector. Electrons fill states up to the Fermi level, with density of states $N(E_k)$ proportional to $\sqrt{E_k}$.

An incoming primary electron interacting with the free electron gas may either excite a single electron to above the Fermi level, or a collective vibration (plasmon). A plasmon may be excited if $E_1 \geq \hbar\omega_p$.

The response of a free electron gas to an external electric field is characterised by $\tilde{\epsilon}$. The imaginary part of $\tilde{\epsilon}$ describes the attenuation of the electric field; it describes the process of energy transfer from the primary electron to the electron gas. Since the intensity of the electric field entering the solid decreases by a factor of $|\tilde{\epsilon}^2|$, the efficiency of energy transfer is given by:

$$\frac{\epsilon_2}{|\tilde{\epsilon}|^2} = -\mathrm{Im}\left(\frac{1}{\tilde{\epsilon}}\right)$$

This function is often referred to as the "Bulk loss". A maxima in the bulk loss is indicative of a high probability for primary electrons to inelastically scatter from the free electron gas.

3.1.4 Implementation of Total Current Spectroscopy Experiment

As part of this project, we designed and built most of the electronics for an automated Total Current Spectroscopy setup. Figure 3.4 shows a block diagram illustrating the key components of the setup. Figure 3.5 shows the circuit diagram for control of the electron gun. Due to the limited range of available power supplies, our experiment has focused on the surface peak of the samples.

In order to automate TCS experiments, both Digital to Analogue and Analogue to Digital Convertors were required (DAC and ADC). To provide these, a custom DAC/ADC Box was designed and constructed. The box can be controlled by any conventional computer with available RS-232 serial communication (COM) ports. The full design of both hardware and software is available on request.

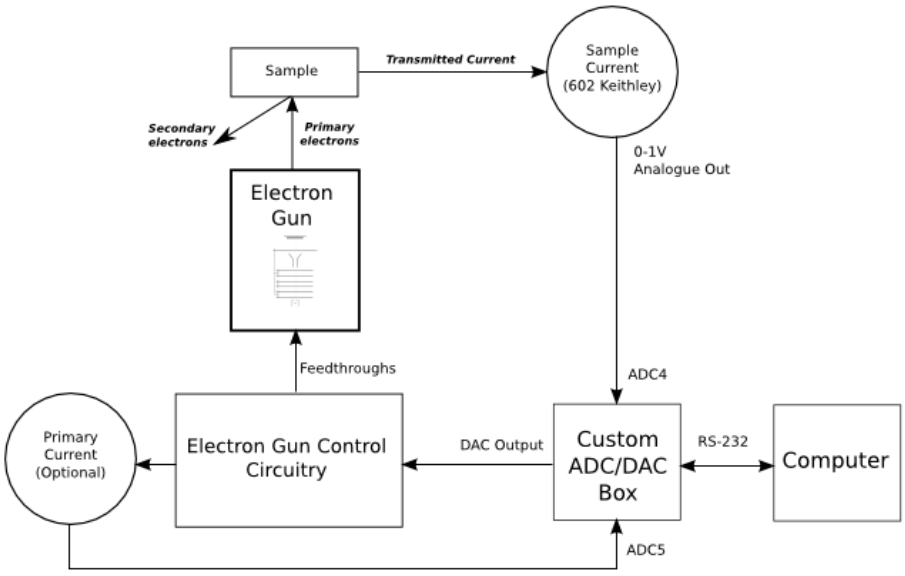

Figure 3.4: Block diagram for TCS setup

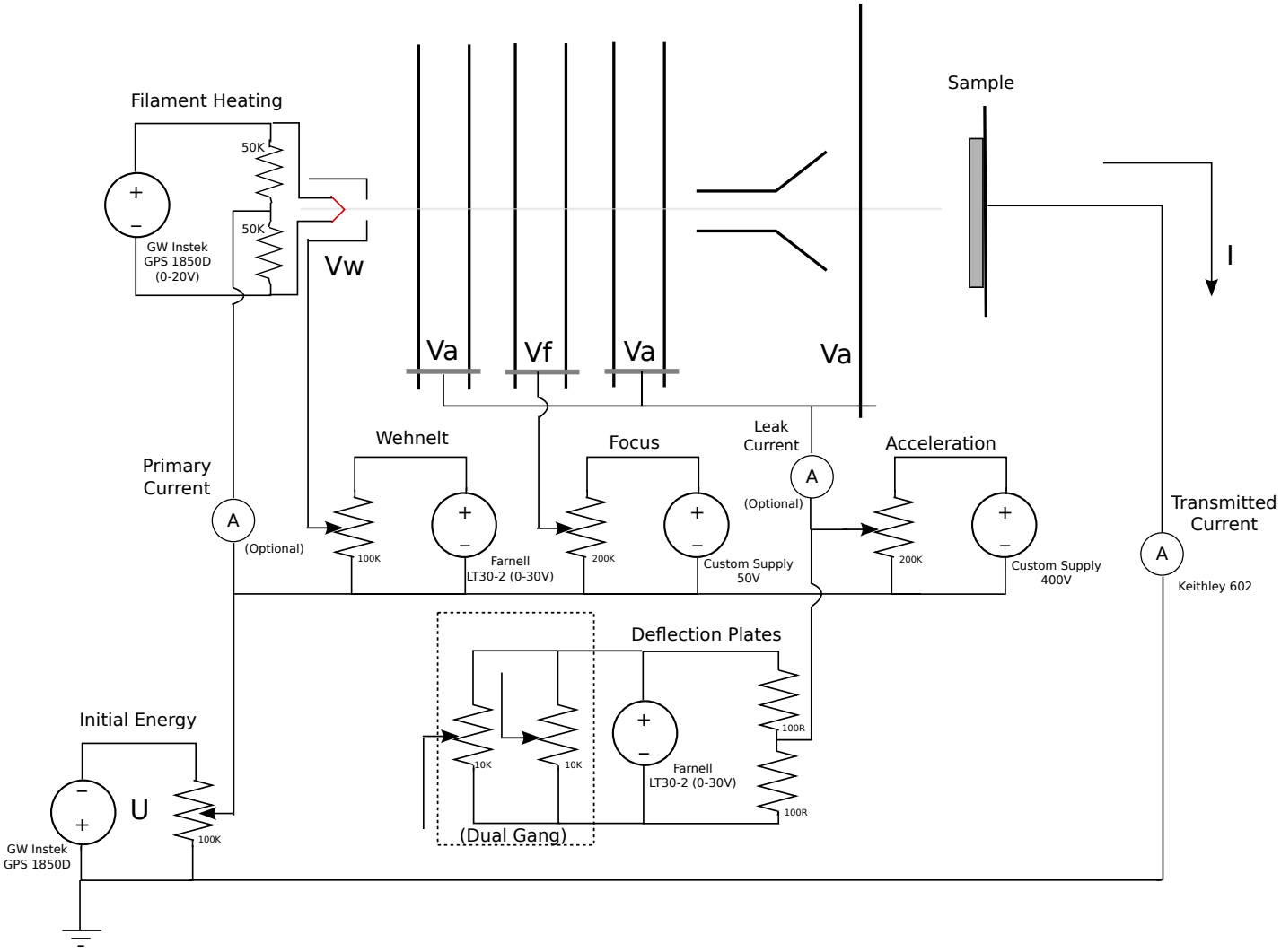

Figure 3.5: TCS circuit diagram

3.2 Ellipsometry

Ellipsometry is a versatile optical technique which can be used to gain a great deal of information about optical and structural properties of thin films. In particular, Ellipsometry may be used to determine the pseudo-dielectric constant $\tilde{\epsilon}$ of a sample. This makes ellipsometry a useful complementary technique to secondary electron spectroscopy experiments, where $\tilde{\epsilon}$ is important for descriptions of electron-electron interactions.

An ellipsometer is designed to establish a beam of light with known polarisation, and measure the change in polarisation due to reflection of the light from a surface. This change in polarisation can be related to the optical properties of the surface, or the thicknesses of a multi-layered sample.

In the Jone's formalism, polarisation states may be represented by orthogonal electric field components E_p and E_s, which are polarised parallel and perpendicular to the plane of incidence respectively. The reflection of a polarised light ray from the surface is described by the matrix equation:

$$\begin{bmatrix} E_{rp} \\ E_{rs} \end{bmatrix} = \begin{bmatrix} r_{pp} & r_{ps} \\ r_{sp} & r_{ss} \end{bmatrix} \begin{bmatrix} E_{ip} \\ E_{is} \end{bmatrix}$$

Where $\boldsymbol{E}_i$ and $\boldsymbol{E}_r$ are the incident and reflected rays. Each element of the 2×2 matrix r_{ij} is the reflection coefficient for i polarised light due to incident j polarised light; these values are generally complex to include the phase change.

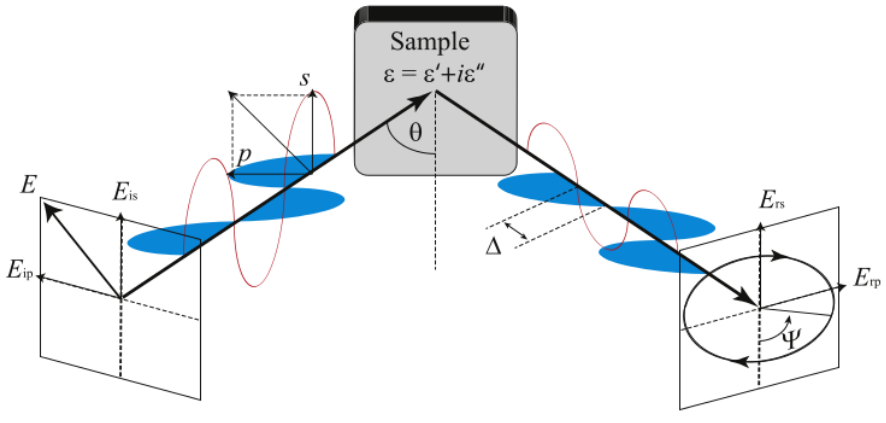

Figure 3.6: Illustration of an ellipsometric measurement [18]

As shown in figure 3.6, linearly polarised light incident upon a surface is in general reflected as elliptically polarised light. For an isotropic sample, $r_{ps} = r_{sp} = 0$, and

we can write $r_{pp} \equiv r_p$ and $r_{ss} \equiv r_s$. A standard ellipsometric measurement expresses the ratio of the p and s reflection coefficients in terms of the two parameters ψ and Δ

$$\tan(\psi)e^{i\Delta} = \rho = \frac{r_p}{r_s} \tag{3.3}$$

The value of $\tan(\psi)$ gives the ratio of amplitudes between the p and s components of the reflected electric field, whilst Δ gives the phase difference.

For an anisotropic sample, ψ and Δ alone are not sufficient to characterise the sample; three seperate ratios of fresnel reflection coefficients are required. Non-uniform films or backside reflection from a substrate may cause the reflected beam to be partially polarised. As a result, the Jone's formalism is not sufficient for characterisation of these samples, and the more general Stokes formalism (which uses 4 component vectors to describe polarisation states) must be employed [29] [18].

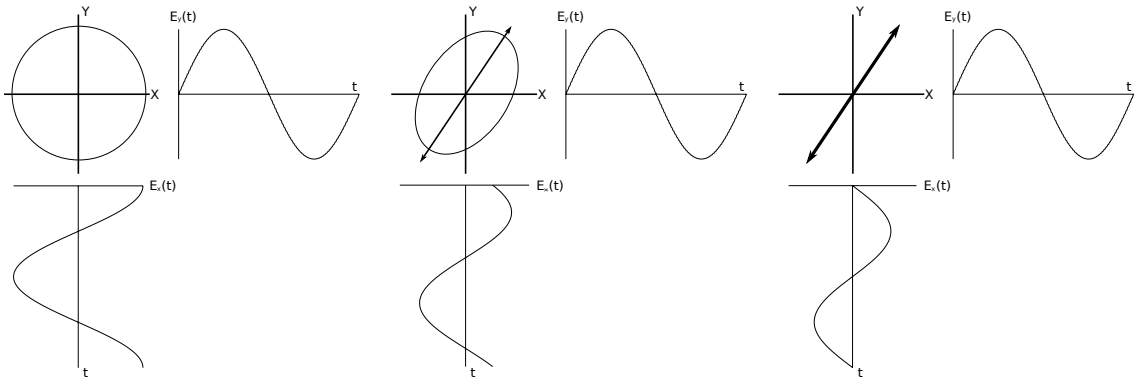

Figure 3.7: From left to right, circular, elliptical and linearly polarised light, viewed along the wavevector of the light

3.2.1 Relation of measurements to properties of the sample

Bulk Optical Constants

The simplest sample is a flat substrate of infinite thickness. In this case, the optical constants of the substrate can be determined directly from ρ:

$$\tilde{\epsilon} = \epsilon_1 + i\epsilon_2 = \sin^2(\phi)\left(1 + \tan^2(\phi)\frac{1-\rho}{1+\rho}^2\right)$$

Where $\tilde{\epsilon}$ is the psueodo-dielectric function. The complex refractive index of the material can be easily related to $\tilde{\epsilon}$:

$$\tilde{\epsilon} = \tilde{n}^2 = (n + i\kappa)^2$$

Where n is the refractive index, and κ is the extinction coefficient.

Multi-layered Samples

At each layer in a multi-layered film, light is be both reflected and transmitted. The measured signal is the result of interference between reflections from each layer. The phase difference for each component of the beam is determined by both the optical constants and the thicknesses of the layers through which the component has passed.

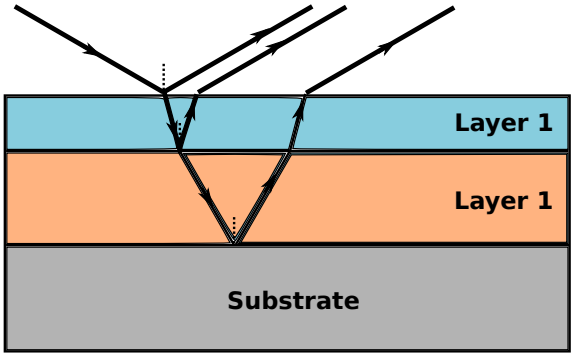

Figure 3.8: Interaction of light with a multi-layered sample

A Note on Si Substrates

A real substrate stored in laboratory air will generally have thin surface layers of oxides. For example, most of the thin film samples produced for this study were prepared on Si substrates. The inclusion of a layer of SiO_2 between the Si substrate and the thin film was found to have a significant effect on the accuracy with which the properties of the sample could be fit.

3.2.2 Variable Angle Spectroscopic Ellipsometry

Although Ellipsometers have been in use for thin film analysis since the late 19th century, traditional instruments were usually limited to single angle and single wavelength measurements, due to the painstaking manual process involved in repeated measurements [30]. With advances both in software and hardware during the last half of the 20th century, Ellipsometric measurements have become largely automated, allowing for a huge number of measurements to be easily obtained from a sample [31, 29].

Spectroscopic Ellipsometry obtains measurements for a range of wavelengths of the incident light. A Variable Angle Spectropic Ellipsometer (VASE) repeats measurements over a range of different angles of incidence. Because of the wealth of data aquired, these techniques are well suited to numerical analysis and fitting procedures to determine both the optical constants and thickness of unknown samples.

At CAMSP a Variable Angle Spectroscopic Ellipsometer (VASE)[2] and the associated software (WVASE32) have been employed in the analysis of thin film samples. Figure 3.9 shows a block diagram of the VASE.

The WVASE32 software allows for the construction of a model of a given sample, using tabulated literature values for optical constants, and allowing the user to specify film thicknesses. This model can then be adjusted using mean square error minimisation fitting algorithms to determine the thicknesses and/or optical constants for the model which best match the measured data. The modelling procedure is illustrated in Figure 3.10.

[2] J. A. Woolam and Co

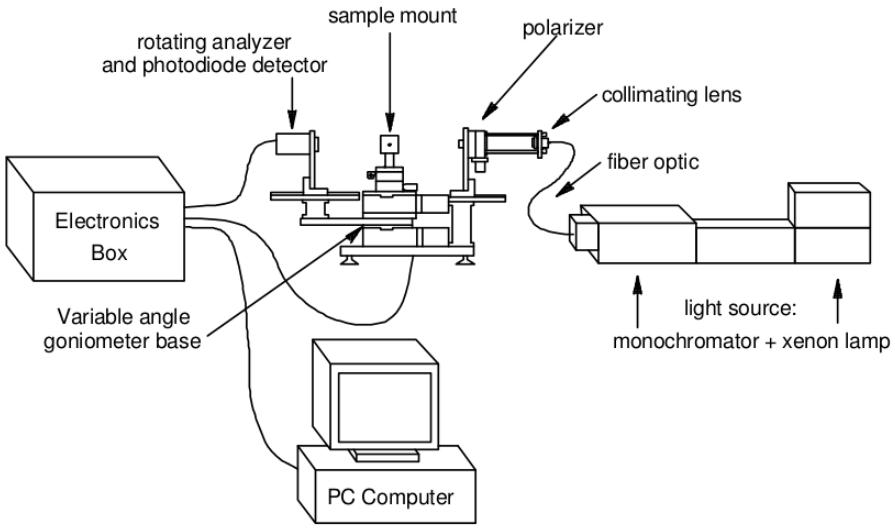

Figure 3.9: Block diagram of the VASE [31]

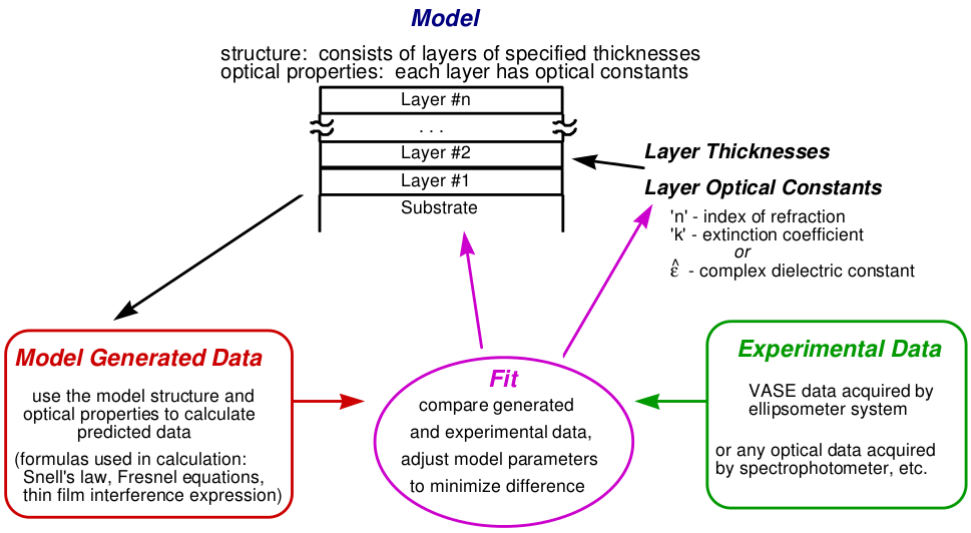

Figure 3.10: Illustration of the VASE analysis and modelling procedure [31]

3.3 Vacuum Techniques and Sample Preparation

All samples required for this study were prepared using available equipment at CAMSP. A small (approx. 25L) vacuum chamber, which has been used previously for thin film preparation at CAMSP [32] was repurposed to allow for both deposition of metallic thin films, and subsequent study using total current spectroscopy. A diagram of this setup is shown in Figure 3.11.

A rotatable stainless steel sample holder was positioned in the centre of the

vacuum chamber. A flange containing evaporators was placed on one side of the chamber, whilst the electron gun required for total current spectroscopy was placed directly opposite. Shielding was used to ensure the electron gun was not coated during deposition. Two sample holders were attached to either side of the shielding to allow for preparation and study of two samples without the need for venting the vacuum chamber.

The evaporators consisted of a tungsten wire filament (diameter 0.5mm) attached using spot welds between two feedthroughs. A piece of the desired metal was folded over the apex of the tungsten wire. The metal was then heated by passing a current through the filament; at sufficiently high currents, the metal piece began to evaporate, with a proportion of the flux of evaporated particles striking the target sample. To remove any contaminating layers from the metal, and ensure uniform evaporation, this procedure was first performed at low pressure (below 10^{-6} mbar) with no sample in the chamber, with the current increased until the metal piece began to melt and form a ball on the wire.

This study focused primarily on depositing Au and Ag films on Si substrates (approx 10x10x3mm wafers), at both high and low pressures. To remove any organic layers, the substrates and sample holders were cleaned in an acetone bath immediately prior to insertion in the vacuum chamber. The thickness of the deposited layer was controlled by varying both deposition time and the heating current.

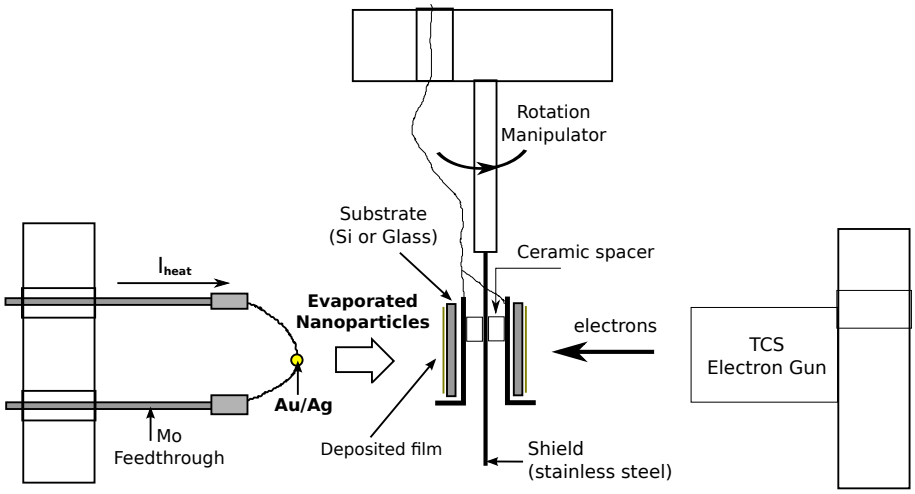

Figure 3.11: Layout of apparatus within the vacuum chamber

Chapter 4

Experimental Results and Discussion

4.1 Scanning Electron Microscopy

A number of samples of black and non-black metal films were prepared and sent to the Centre for Microscopy Characterisation and Analysis (CMCA) at UWA for study. In this section we will present and discuss two of the images produced by CMCA. These images proved to be an invaluable aid in understanding the structural differences between metallic-black and metallic-bright films.

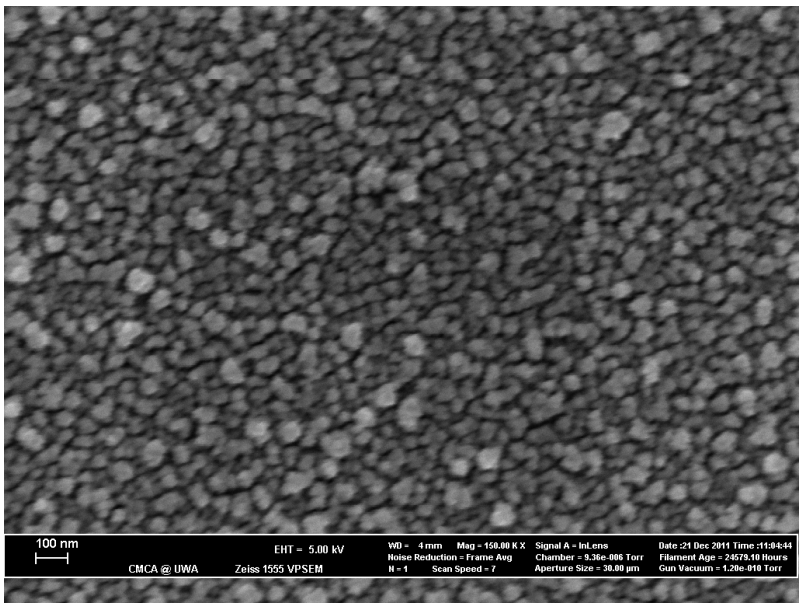

Figure 4.1: SEM Image of a Au film. Pressure of preparation 10^{-6} mbar. Dimensions approx. 2500 x 1900 nm

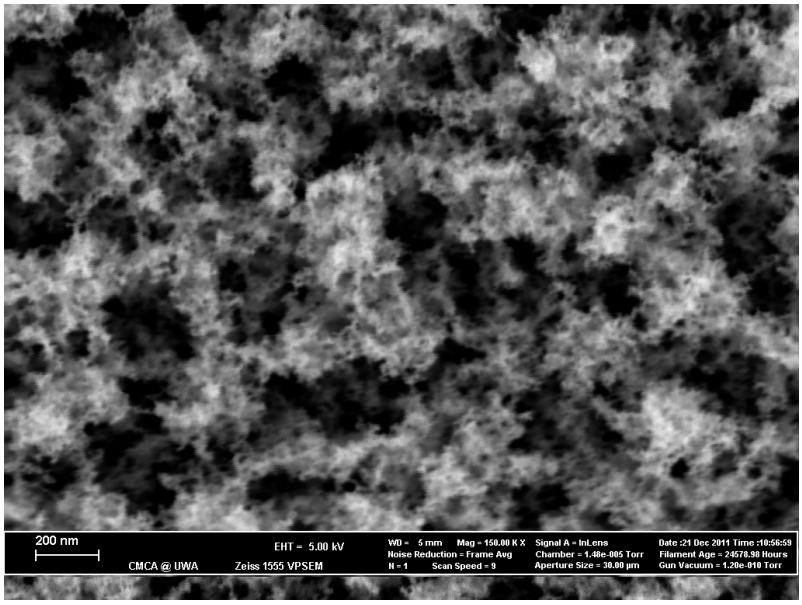

Figure 4.2: SEM Image of a Black Au film. Pressure of preparation 0.18 mbar. Dimensions approx. 2500 x 1900 nm

Figures 4.1 and 4.2 shows a comparison of a Black Au and a Au film imaged using a scanning electron microscope (SEM). The structural difference between the two films is striking. The surface of the Au film appears to consist of a layer of well defined metallic nanoparticles with sizes ranging from 20 to 100nm. In contrast, the Black Au film shows a highly irregular, patchlike pattern. Previous studies have produced similar SEM images [2, 3, 14].

Intensity distributions of the SEM images (Figure 4.3) show a smooth gaussian like peak for the Au film. In contrast, the intensity distribution of the Black Au film reveals an extremely high maxima at zero intensity, indicating that most of the surface has a very low secondary electron emission coefficient. The tail of this distribution is very flat, and extends to high intensity values, consistent with the observed patch like regions of high intensity values.

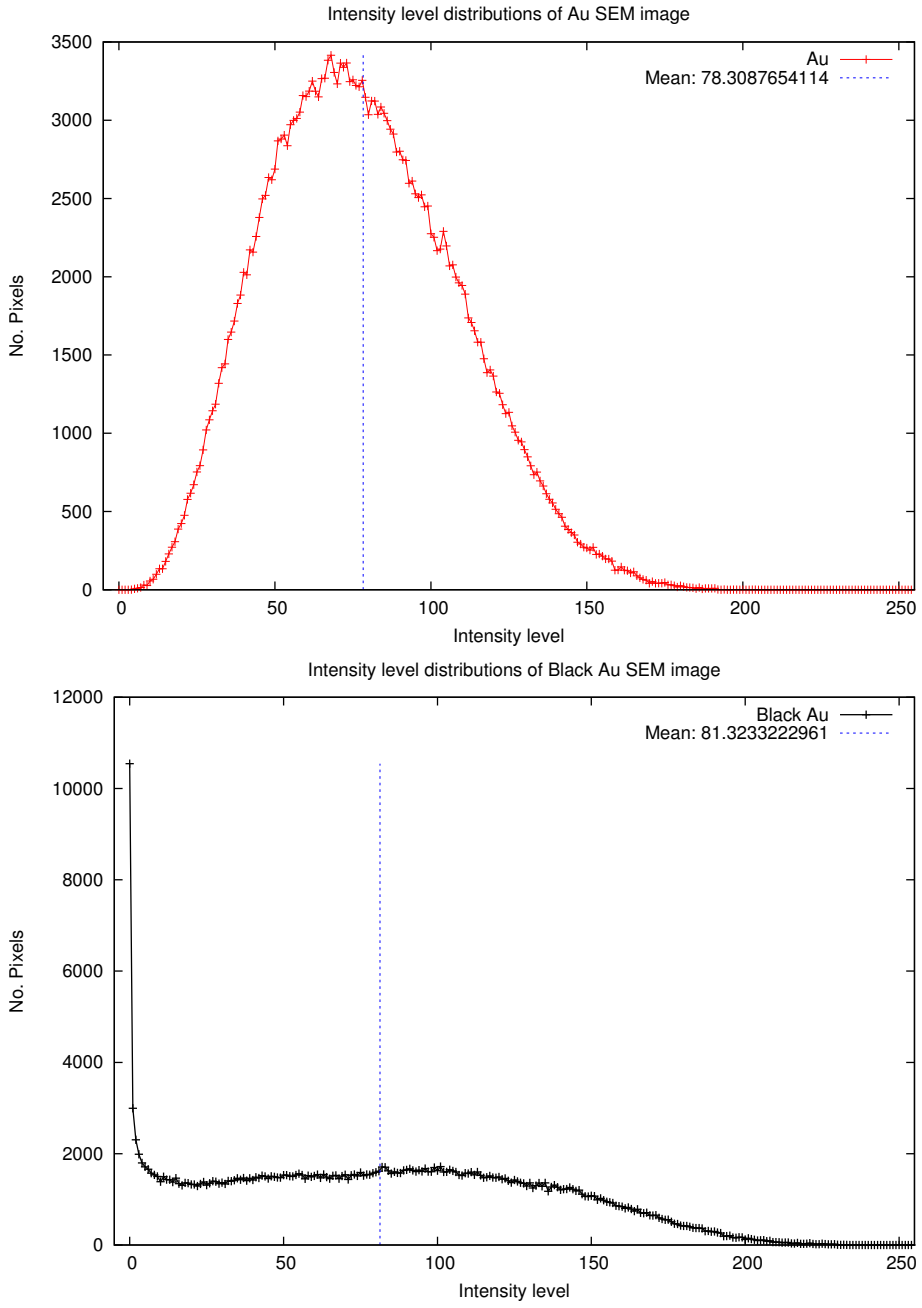

Figure 4.3: Intensity distributions for the SEM images in Figures 4.1 and 4.2. The total number of pixels for each intensity level (0-255) is shown. Similar analysis have been performed by Panjwani [3].

4.2 Total Current Spectropy

4.2.1 Tuning the Electron Gun

In 3.1, it was assumed that all primary electrons were incident normal to the surface, with an energy distribution $f(E - E_1)$ determined by the cathode. In reality, the primary beam has both angular and energy distributions. One can think of the cathode as producing initial angular and energy distributions, which are altered by the focusing properties of the electron gun to produce the distributions at the sample.

As discussed in 3.1, the effective energy distribution of primary electrons appears at the contact potential as the first peak in $S(U)$. Any peaks due to inelastic processes are convolved with the effective energy distribution. If the angular distribution is not centred about $\theta_1 = 0$ (due to misalignment of the sample holder) the observed contact potential is increased. Therefore it is desirable to adjust the electron gun so as to produce the narrowest possible distribution, at the lowest possible contact potential. In Figure 4.4 we show the adjustment of the central electrodes to minimise the width of the elastic scattering peak.

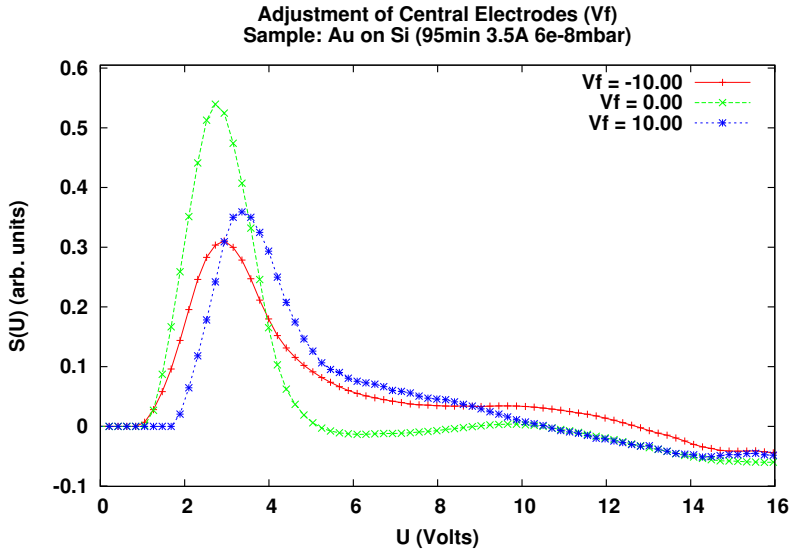

Figure 4.4: Adjusting the central electrodes to optimise the effective energy distribution

4.2.2 Electron gun simulation

Figures 4.5 and 4.6 show the results of an electron gun simulation written for this project. The results of this simulation were not used to focus the actual electron gun; however Figure 4.5 was useful, as it shows the possibility for electrons to strike the insulating posts holding the gun together. An insulating material in the path of the electron beam would become charged over time, and affect the focusing properties of the gun. When these posts were covered with tantalum strips connected to the final electrode, the stability of the measured current at fixed U was improved.

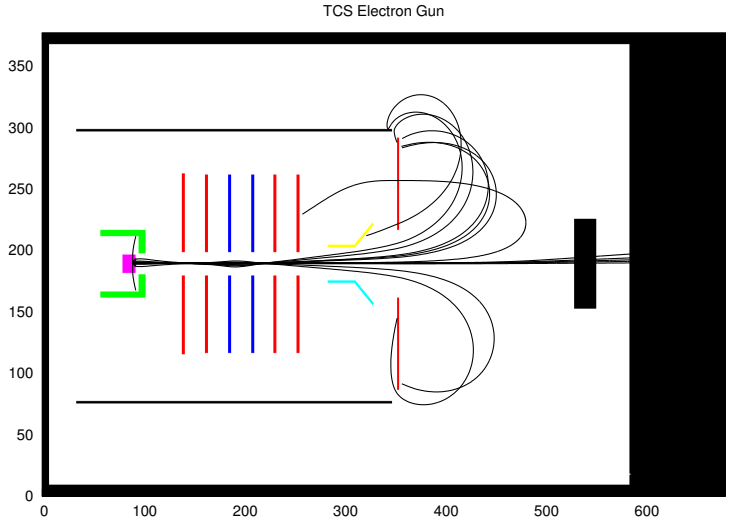

Figure 4.5: Simulated electron trajectories

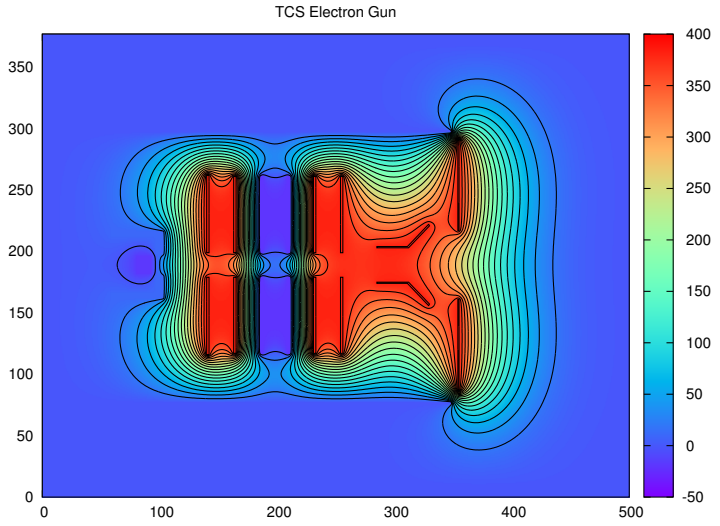

Figure 4.6: 2D Simulation of the electrostatic potential produced by the electron gun

4.2.3 Deposition of Ag films onto a Si substrate

We have measured the total current spectra for Ag films deposited onto an Si substrate. An optically thick layer of Ag, followed by a thin layer of Black Ag [1] were deposited, with measurements performed before and after each deposition.

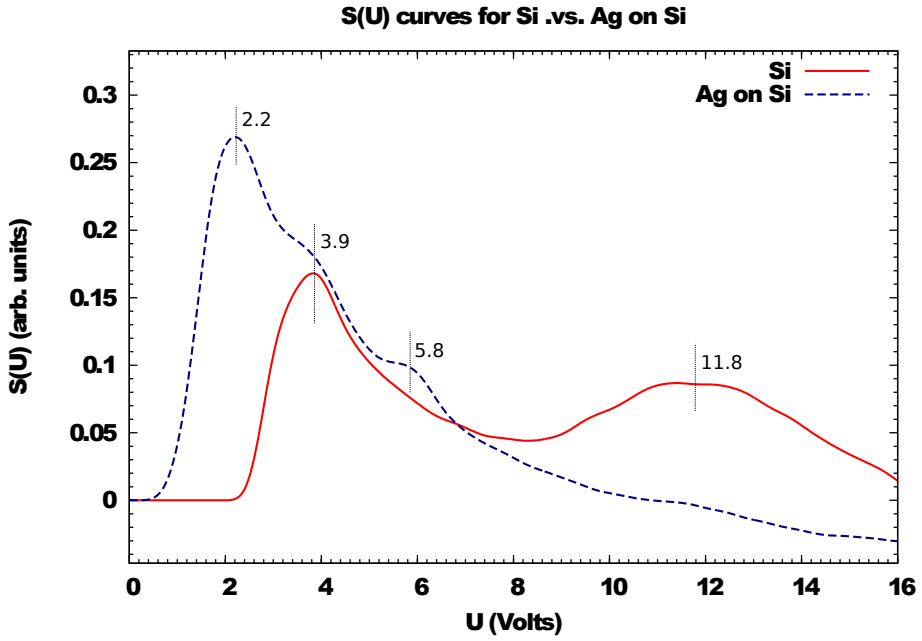

Figure 4.7: Comparison of Si and Ag on Si TCS

In Figure 4.7, the total current spectrum of the sample changes dramatically with the Ag deposition. The contact potential of the surface decreases by about 1.7V. Typical literature values for Si and Ag work functions would predict a shift of at most $4.9 - 4.2 = 0.7$V. In interpreting this shift it is important to note that our surfaces are not atomically clean.

Ellipsometric measurements had found that the Si substrates used in this study had SiO_2 surface layers with thicknesses of several nanometers. Comparing literature values for Ag and SiO_2 work functions shows that the expected difference in contact potentials for an Ag and SiO_2 is between 0.8V and 1.8V[2].

In addition to the change in contact potential of the surface, an inflection point is visible in the Ag spectrum at the location of the contact potential for SiO_2. Even though the Ag sample was optically thick, it seems that the surface potential of the underlying SiO_2 layer may still be contributing to $S(U)$.

[1] pressures approx 10^{-7} and 0.18mbar respectively

[2] The exact values of the work functions depend upon the orientation of the crystal lattice at the surface layer and shape of the Fermi-surface of the material

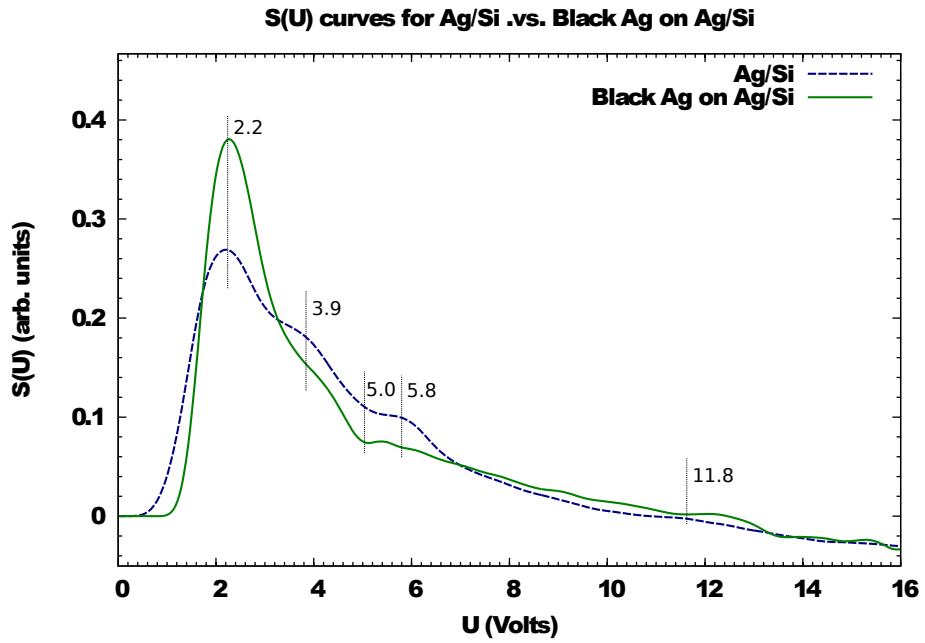

Figure 4.8: Comparison of Ag/Si and Black Ag on Ag/Si spectra

Figure 4.8 shows the change in TCS after a layer of Black Ag is deposited on the existing Ag layer. The contact potential of the surface changes only slightly. This is unsurprising, as the new surface layer consists mostly of the same material. However, the surface peak has narrowed, despite no change in the focusing of the electron gun. This change in surface peak may be attributed to a change in the surface potential of the sample after the Black Ag layer was deposited. In particular the surface peak has narrowed, which is indicative of either a sharper potential barrier at the surface, or a more uniform potential accross the irradiated surface area.

Our experimental setup has been limited to applied potentials of 0 to 16V. The contact potentials of the surfaces have limited the range of primary electron energies to just over 10 eV. Referring to Figure 3.2 (which is idealised), it is recommended that this range be extended if the experiment were to be used for study of inelastic scattering processes.

4.3 Optical Transmission Spectroscopy

In the transmission spectroscopy experiments, white light has been shone through a thin metallic film mounted on a glass slide. A commercial visible range optical

spectrometer[3] was used to measure the spectrum of the transmitted light in comparison. The transmission of a sample can be determined after first measuring the spectrum of the white light source. For thin films on a glass substrate, the transmission spectrum may be estimated after first determining the transmission spectrum of the glass.

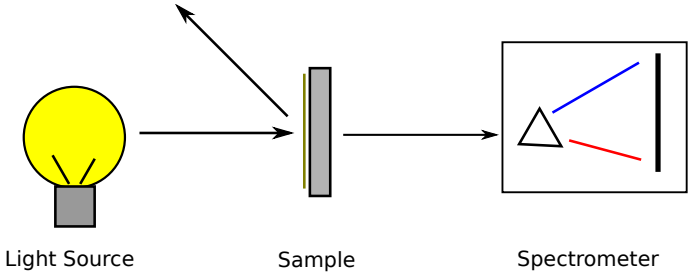

Figure 4.9: Setup for a transmission spectroscopy experiment

A 653nm filter was used to test the response of the spectrometer. The measured wavelength for peak transmission was 650.8nm. The stated uncertainty in the filter's peak transmission wavelength was ±2% (approx. 13nm).

4.3.1 Reference Spectrum

The Ellipsometer's Xe Arc Lamp was used as a light source. Its spectrum $I_0(\lambda)$ is shown in Figure 4.10. This measurement established that the Xe Arc lamp was indistinguishable from background light levels below $\lambda \approx 320$nm.

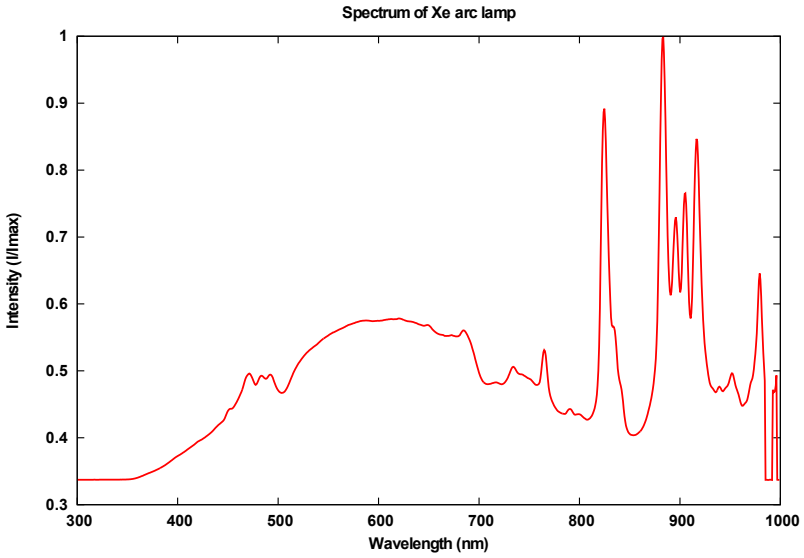

Figure 4.10: Xe Lamp reference spectrum

[3]OceanOptics QE65000

4.3.2 Transmission Spectra of Au and Black Au on Glass

Transmission spectra for similar thickness Au and Black Au films were measured, accounting for the transmission of the glass and the reference spectrum.

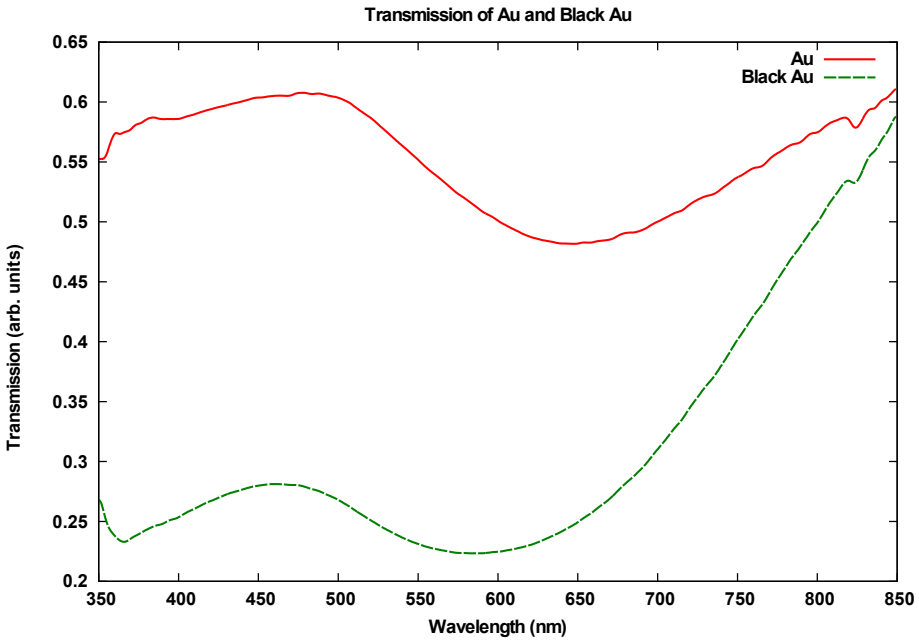

Figure 4.11: Transmission Spectra of Au and Black Au films

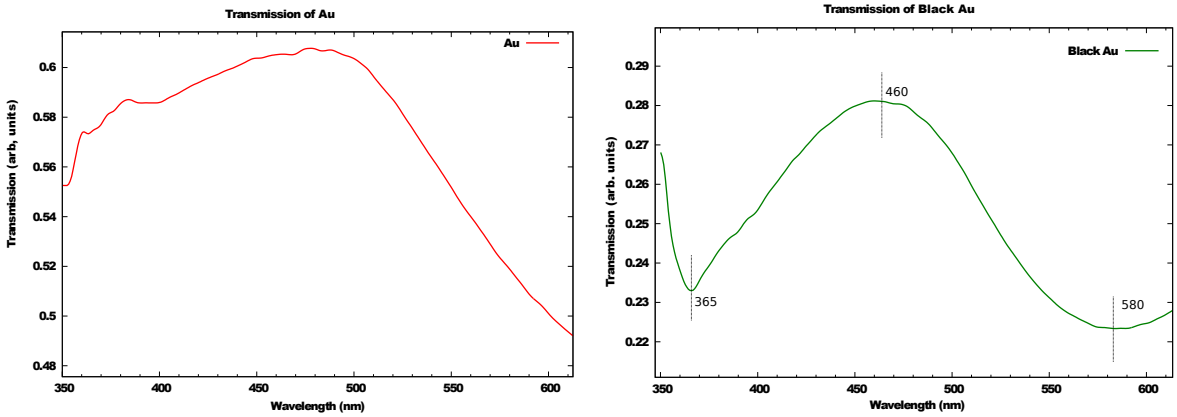

Figure 4.12: Transmission Spectra for $\lambda \leq 620$nm

The results show that Black Au is far less transmissive than Au in the visible part of the spectrum. Both spectra reveal a similar double peak shape. As found by Pfund and other researchers, the transmission of the Black Au film increases into the infra-red part of the spectrum[15, ?, 13]. There are particularly interesting differences near 350nm. The Black Au film shows a dip in transmission which is notably absent in the Au film.

4.4 Variable Angle Spectroscopy Ellipsometry

4.4.1 Model for Ag and Black Ag on a Si substrate

Testing showed that it is difficult to use Ellipsometry to characterise black metal films of considerable thickness (estimated $> 30nm$), due to the extremely low reflectivity of such films. However, using the WVASE32 software, it was possible to fit for the optical constants of an extremely thin layer of Black Ag prepared on Si using ellipsometric measurements. Figures 4.13 and 4.14 show the fitted optical constants for the Ag layer in a multilayered model for both a Black Ag thin film, and Ag thin film. Bulk Ag optical constants from Palik's Handbook [33] were specified for the initial values.

The models include an SiO_2 surface layer, with the thickness fit. The EMA layer models the effect of surface roughness in the film. This layer uses the Bruggeman model to describe the surface as a set of spherical inclusions of the Black Ag material in a void. The Bruggeman EMA formula is [34, 18]:

$$F\frac{\epsilon_b - \epsilon_{eff}}{\epsilon_b + 2\epsilon_{eff}} + (1-F)\frac{\epsilon_c - \epsilon_{eff}}{\epsilon_c + 2\epsilon_{eff}} = 0$$

where ϵ_b and ϵ_c are the dielectric functions of the two materials (in our case, material b is air; $\epsilon_b = 1$), and F is the volume fraction of material b. This model is incorporated into the WVASE32 software.

Although from SEM images it is clear that the structure of Black films is far more complicated than this approximation, fitting for the fraction of Black Ag in the surface layer shows a majority of the surface is empty. This is consistent with the porous nature of Black metal films seen in SEM images. The thickness of this layer was also a free parameter in the model.

Both the refractive index and extinction coefficient of the Black Ag film show a strong peak around 370 nm. From the refractive index, the Black Ag film has a much stronger dispersion relation than the Ag film. The extinction coefficient peak indicates a preferential scattering or absorbsion of light at 370 nm. This may be indicative of surface plasmon resonance effects [18, 35, 36], particularly since it occurs near to the bulk plasmon frequency for Ag. It is interesting to note that the peak in extinction for the thin Ag film occurs within 30 nm of the dip in transmission measured for an Au film (Figure 4.12).

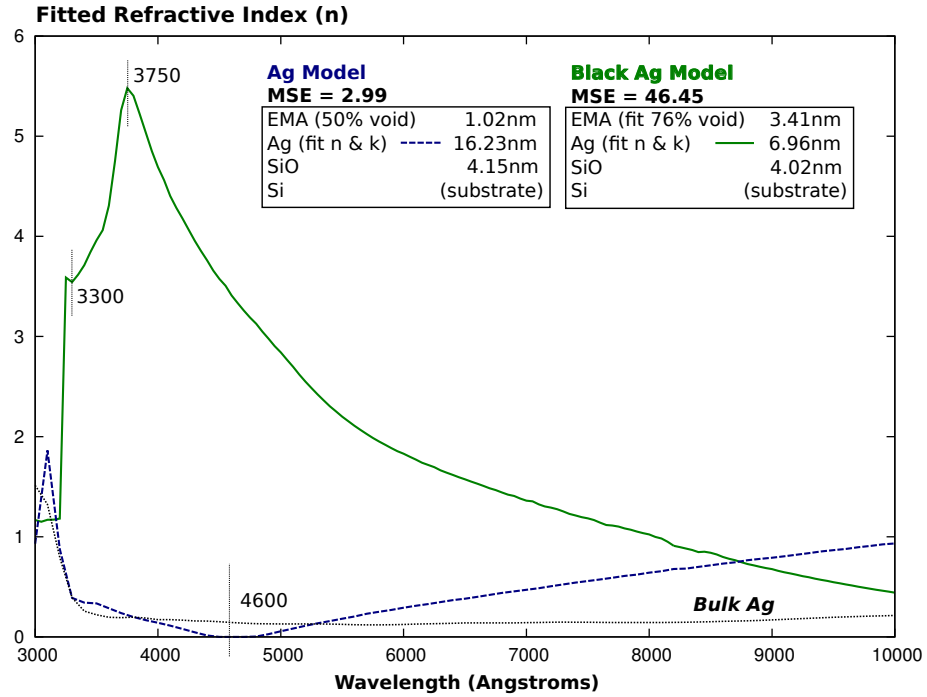

Figure 4.13: Fitted refractive index for the Ag layer in multilayered models for Ag and Black Ag (step size 50 nm)

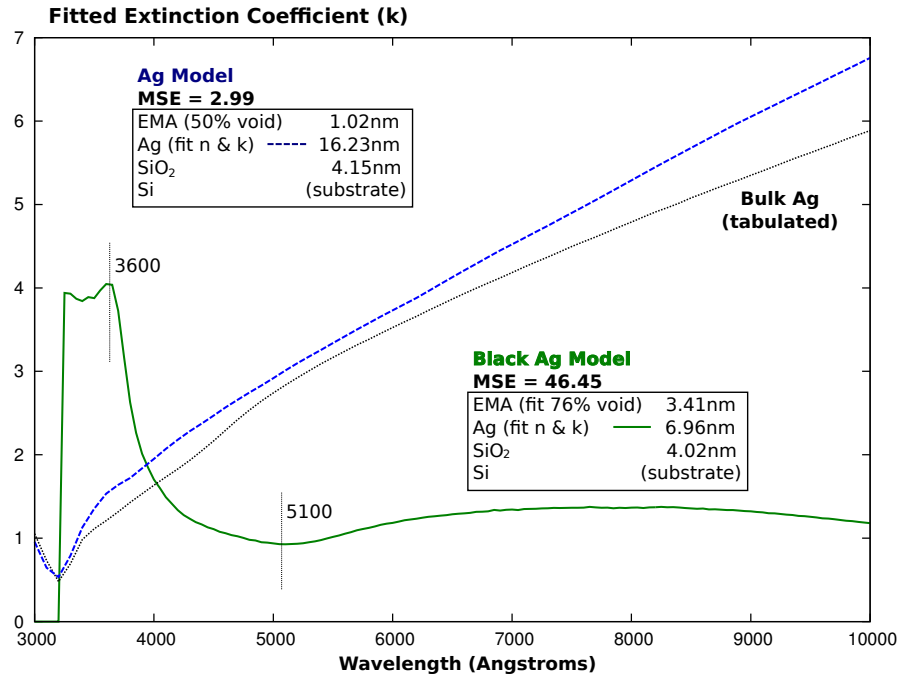

Figure 4.14: Fitted extinction coefficient for the Ag layer in multilayered models for Ag and Black Ag (step size 50 nm)

4.4.2 Surface and Bulk Plasmons in the Ag and Black Ag films

The bulk loss function as introduced in Section 3.1.3 is:

$$L_b = -\mathrm{Im}\frac{1}{\tilde{\epsilon}}$$

The occurance of maxima in L_b can be used as a condition for determining bulk plasmon excitation frequencies [27].

For surface plasmon excitations, the surface loss function is [37]:

$$L_s = -\omega \mathrm{Im}\left(\frac{1}{1+\tilde{\epsilon}}\right)$$

When applied to the thin Ag film (Figure 4.15) the bulk loss function shows a strong peak at 320nm, and is otherwise rather flat. This peak corresponds to the bulk plasmon frequency for Ag ($\hbar\omega_p \approx 3.8$eV. It should be noted that the stated uncertainty of Ellipsometric measurements is above 20% for wavelengths below 320nm. In addition we initially specified the film to have bulk optical constants, for which this result is to be expected.

When the bulk and surface loss functions are applied to the Black Ag film (Figure 4.16), there is in fact a shallow minima at 370nm. In contrast to the Ag film, the loss functions appear to increase monatomically for longer wavelengths.

Based upon these results, we cannot conclude that this particular Black Ag film will support surface or bulk plasmon oscillations. However, we cannot rule out that localised plasmonic resonance effects contribute to a scattering of light causing the peak in k around 3800. Due to the complicated structure of the surface it would be difficult to theoretically describe the nature of such effects. A starting point for future theoretical work may be Harris' models of black metal films as a series of interwoven conducting strands [2].

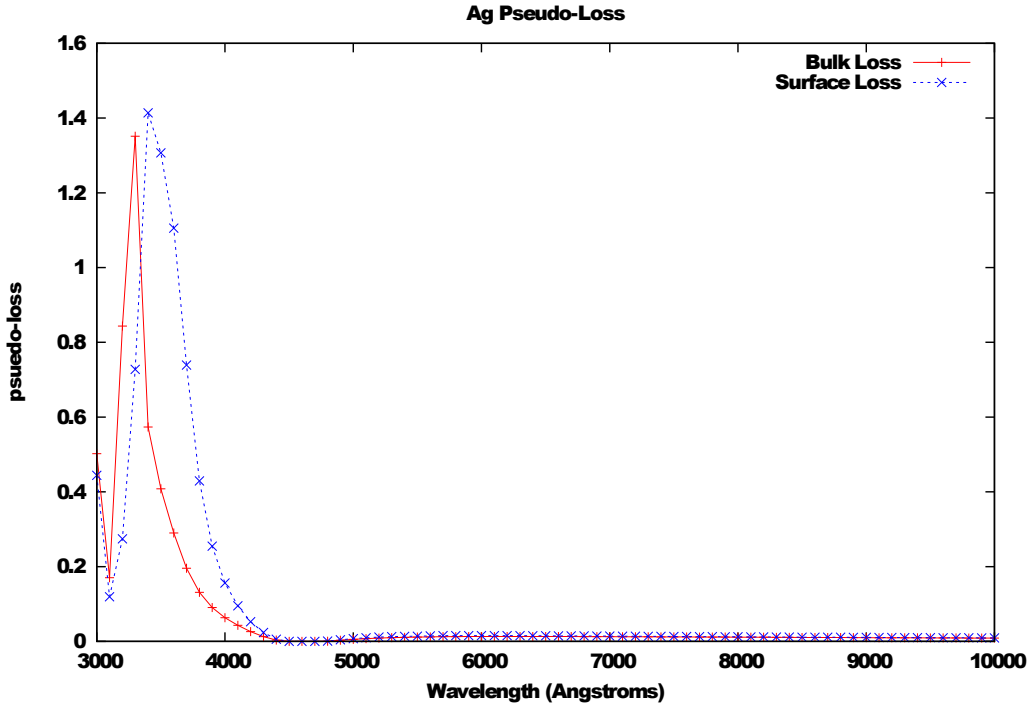

Figure 4.15: Pseudo-loss functions for the Ag thin film

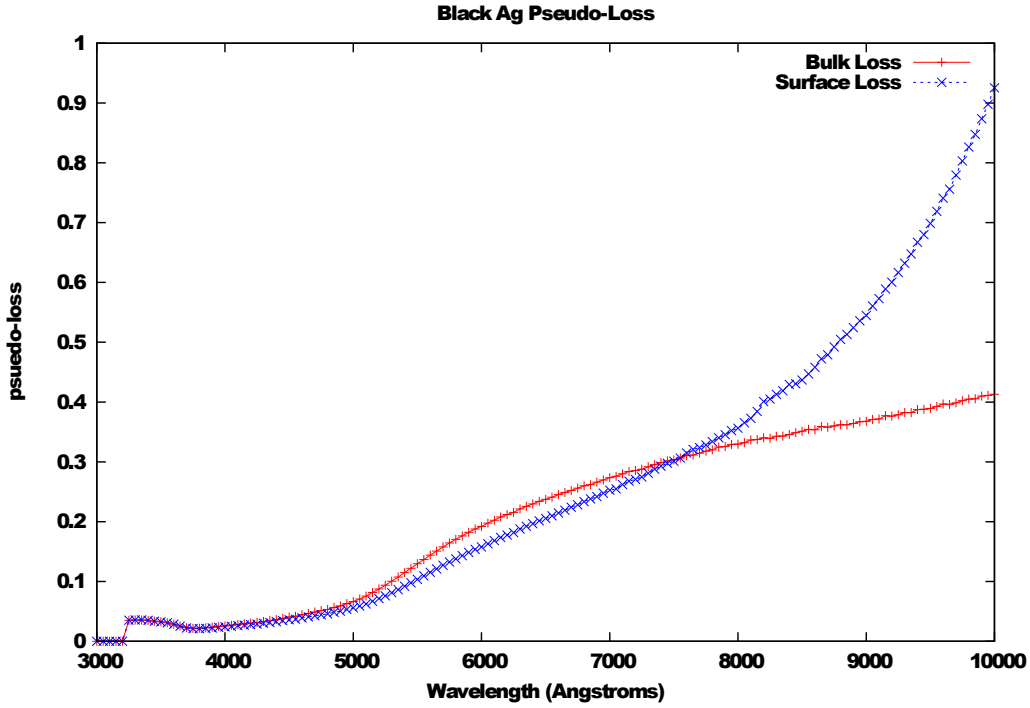

Figure 4.16: Pseudo-loss functions for the Black Ag thin film

Chapter 5

Conclusions

1. We fabricated a range of nanostructured metallic thin films on both Si and glass substrates using evaporative techniques. These films have been characterised using a combination of electronic and optical spectroscopy techniques.

2. Secondary electron microscopy analysis reveals striking differences in the structure of Au and Black Au films; Au films have been shown to consist of a regular periodic array of nanoparticles, whilst Black Au appears to consist of a highly randomised, porous mix of strand like structures.

3. A Total Current Spectroscopy experiment for characterisation of samples in situ has been integrated with the technology for sample preparation. We used this setup to investigate elastic scattering of electrons as a function of film deposition.

    - Results for Black metal films deposited on existing layers of metal films suggest that the Black metal films present a sharper, more step like potential barrier to the primary electrons.
    - Further improvements may be made to the Total Current Specroscopy experiment with a possibility to investigate inelastic scattering processes occuring in the metallic thin films.

4. The optical properties of Black Au have been investigated and compared with those of Au.

    - Transmission spectroscopy experiments support existing evidence for a plateau in the infra-red.

- We found a minima in the transmission spectrum of a Black Au film at around 370nm; this minima is absent in the spectrum of a similar thickness Au film.

5. Ellipsometry has been used to determine the optical constants of thin films of Ag and Black Ag. These results show a significant peak in both the refractive index and extinction coefficient of the Black Ag film in the region of 350 to 400nm. These peaks are absent for the Ag sample.

References

[1] A. H. Pfund, "Bismuth black and its applications," *Review of Scientific Instruments*, 1930.

[2] L. Harris and J. K. Beasley, "The infrared properties of gold smoke deposits," *Journal of the Optical Society of America*, 1952.

[3] D. R. Panjwani, "Metal blacks as scattering centers to increase the efficiency of thin film solar cells (thesis)," *Department of Physics, University of Central Florida*, 2011.

[4] M. Faraday, "Experimental relations of gold (and other metals) to light," *M Philosophical Transactions of the Royal Society of London (1776-1886)*, 1857.

[5] M. Garnet *Philosophical Transactions of the Royal Society A*, vol. 203, pp. 385–420, 1904.

[6] G. Mie, "Beirtrage zur optik truber medien, speziell kolloidaler metallosungen," *Ann. Phys. (Leipzig)*, vol. 25, 1908.

[7] T. Wriedt, "Mie theory 1908-2008 - introduction to the conference," *(Conference) Mie Theory 1908-2008 - Present developments and Interdisciplinary aspects of light scattering*, 2008.

[8] H. A. Atwater and A. Polman, "Plasmonics for improved photovoltaic devices," *Nature materials*, 2010.

[9] P. C. Suljo Linic and D. B. Ingram, "Plasmonic-metal nanostructures for efficient conversion of solar to chemical energy," *Nature Materials*, 2011.

[10] A. R. D. Ivan S. Maksymov and Y. S. Kivshar, "Enhanced emission and light control with tapered plasmonic nanoantennas," *Applied Physics Letters*, 2011.

[11] I. S. Maksymov, "Optical switching and logic gates with hybrid plasmonicphotonic crystal, nanobeam cavities," *Physics Letters A*, 2010.

[12] B. M. S. Louis Harris, Rosemary T. McGinnies, "The preparation and optical properties of gold blacks," *Journal of the Optical Society of America*, 1948.

[13] L. Harris and A. L. Loeb, "Conductance and relaxation time of electrons in gold blacks from transmission and reflection measurements in the far infrared," *Journal of the Optical Society of America*, vol. 43, no. 11, 1953.

[14] D. R. McKenzie, "Selective nature of gold-black deposits," *Applied Optics*, 2006.

[15] A. H. Pfund, "The optical properties of metallic and crystalline powders," *Journal of the Optical Society of America*, 1933.

[16] J. T. C. Donna J. Advena, Vincent T. Bly, "Deposition and characterization of far-infrared absorbing gold black films," *Applied Optics*, 1993.

[17] T. H. Thomas Sndergaard, Sergey M. Novikov, R. L. Eriksen, J. Beermann, Z. Han, K. Pederson, and S. I. Bozhevolnyi, "Plasmonic black gold by adiabatic nanofocusing and adsorption of light in ultra-sharp convex grooves," *Nature Communications*, 2012.

[18] H. A. T.W.H Oats, H. Wormeester, "Characterization of plasmonic effects in thin films and metamaterials using spectroscopic ellipsometry," *Progress in Surface Science (Elsevier Ltd)*, 2011.

[19] R. Ferrell, "Predicted radiation of plasma oscillations in metal films," *Physical Review*, no. 111, pp. 1214–1222, 1958.

[20] C. Kittel, *Introduction to Solid State Physics*. John Wiley and Sons, New York, 7 ed., 1996.

[21] R. H. Ritchie, "Plasma losses by fast electrons in thin films," *Physical Review*, vol. 106, 1957.

[22] D. Bohm and D. Pines, "A collective description of electron interactions. i. magnetic interactions," *Phys. Rev.*, vol. 82, pp. 625–634, Jun 1951.

[23] D. Pines and D. Bohm, "A collective description of electron interactions: Ii. collective vs individual particle aspects of the interactions," *Phys. Rev.*, vol. 85, pp. 338–353, Jan 1952.

[24] D. Pines and D. Bohm, "A collective description of electron interactions: Iii. coulomb interactions in a degenerate electron gas," *Physical Review*, vol. 92, 1953.

[25] C. Powell and J. Swan, "Origin of the characteristic electron energy losses in aluminium," *Physical Review*, vol. 115, no. 4, 1959.

[26] E. V. C. J. M. Pitarke, V. M. Silkin and P. M. Echenique, "Theory of surface plasmons and surface plasmon polaritons," *Reports on Progress in Physics*, no. 70, 2007.

[27] S. Komolov, *Total Current Spectroscopy of Surfaces*. Gordon and Breach Science Publishers S.A, 1992.

[28] L. C. S.A. Komolov, "Total current spectroscopy," *Surface Science*, vol. 90, no. 2, pp. 359–380, 1979.

[29] J. A. Woolam and Co., "Overview of variable angle spectroscopic ellipsometry (vase), part ii: Basic theory and typical applications," *Optical Metrology*, 2000.

[30] H. G. Tompkins, *A User's Guide to Ellipsometry*. Dover Publications, 1992.

[31] J. A. Woolam and Co., "Overview of variable angle spectroscopic ellipsometry (vase), part i: Basic theory and typical applications," *Optical Metrology*, 1999.

[32] N. Kostylev, "Plasmonic excitations in nanostructures (thesis)," *School of Physics, Western Australia*, 2011.

[33] E. P. D.W. Lynch, W.R. Hunter, *Handbook of Optical Constants of Solids*. Academic Press, New York, 1985.

[34] D. Bruggeman, "Calculation of various physics constants in heterogenous substances i dielectricity constants and conductivity of mixed bodies from isotropic substances," *Ann. Phys.-Berlin*, no. 24, p. 636664, 1935.

[35] C. Sonnichsen, "Plasmons in metal nanostructures (dissertation)," *Ludwig-Maximilians-University of Munich*, 2001.

[36] Y. B. Zheng and T. J. Huang, "Surface plasmons of metal nanostructure arrays: From nanoengineering to active plasmonics," *The Association for Laboratory Automation*, 2008.

[37] H. L. H. Ibach, *Solid-State Physics: An Introduction to Principles of Materials Science*. Springer-Verlag, New York, 2010.

Summary of Student Achievements

1. Implementation of a low energy Total Current Spectroscopy experiment, involving:
   - Design and construction of the sample holder
   - Design and construction of the electron gun control circuit
   - Design and construction of an automated data aquisition system (both hardware and software). This system was used to produce over 2GB in data files during the project.
   - Attaching cable plugs for use with the TCS experiment (also, reattaching existing damaged plugs)
   - Implementation of a webcam based system for automatic monitoring of chamber pressure
   - Focusing the electron gun
   - Design and implementation of custom software which assisted in troubleshooting the electron gun
   - Modifications to the electron gun to reduce charging problems
   - Developement of software for analysis and processing of TCS data
2. Preparation of black and non-black nanostructured metal surfaces on both Si and glass substrates
3. Obtaining all ellipsometric measurements for samples
4. Construction of models within the WVASE32 software
5. Design and construction of a sample holder for the transmission spectroscopy experiments
6. Analysis of SEM images prepared by CMCA

B.Sc. (Hons) Physics Project

Research Proposal

Samuel Moore
School of Physics, University of Western Australia
April 2012

Characterisation of Nanostructured Thin Films

Keywords: surface plasmons, nanostructures, spectroscopy, metallic-blacks
Supervisers: W/Prof. James Williams (UWA), Prof. Sergey Samarin (UWA)

1 Research Plan

1.1 Aim

This project aims to explore the electronic and optical properties of metallic nanostructures in thin films. The focus will be on creating structures which exhibit plasmonic effects, and the detection of these effects using various experimental techniques. The samples to be studied will be prepared under vacuum by evaporative deposition, and the effects of environmental conditions and post deposition treatment on the properties of the samples will be investigated. Samples of particular interest include so called "metal-black" films, and multilayered metal structures. Experimental techniques to be used include Ellipsometry, Optical Reflection and Transmission Spectroscopy, and Electron Spectroscopy.

1.2 Significance

An understanding of the properties of nano structures is essential for further progress in the miniaturisation of components of electronic devices and fabrication of functional materials. In particular, the coupling of photons to surface plasmon resonances in nanostructures may hold the key to developing photonic based computer devices [1]. The field enhancement caused by coupling of photons to surface plasmons has also been exploited for many applications including increasing the efficiency of thin film solar cells[2] and reception of light by nanoscale antenna's [3].

1.3 Methods

All work will be undertaken at the Centre for Atomic, Molecular and Surface Physics (CAMSP) in UWA.

1.3.1 Preparation of Samples

Thin films of metallic nanostructures can be produced by several techniques. This project will use evaporative deposition in a vacuum chamber.

The preparation of "metal-black" films requires a "bad" vacuum (10^{-2} mbar). This required pressure will be obtained by pumping the chamber to high vacuum (10^{-7} mbar) with a turbo-molecular pump, before

flooding it with a chosen gas.

1.3.2 Ellipsometric Measurements

Ellipsometry is a versatile technique which can be used to determine not only the optical properties of materials, but also information about their composition and structure. Essentially, Ellipsometry measures the change in polarisation of light reflected from a sample. In the simplest case of a bulk substrate, this can be related directly to the optical constants of the material via the Fresnel equations. In more complex cases a multilayered model must be used, and various optical effects must be considered.[4], [5]

A Variable Angle Spectroscopic Ellipsometer (VASE) is capable of performing ellipsometric measurements across a large range of angles and wavelengths. The huge amount of data acquired is of enormous benefit in obtaining an accurate model for a sample. A VASE belonging to CAMSP will be used for Ellipsometric measurements, and specialised software provided with this Ellipsometer will be used for the modelling of experimental results.

1.3.3 Optical Reflection and Transmission Spectroscopic Measurements

The VASE at CAMSP is also capable of performing reflection and transmission measurements on prepared films for the p and s polarised components of incident light. An advanced spectrometer (OceanOptics) can also be used for performing reflection and transmission measurements.

1.3.4 Electron Spectroscopy

An electron gun will be setup in a vacuum chamber, to allow for the electron spectroscopy application for studying the films deposited in the same vacuum chamber.

To begin with, samples of "metal-black" films will be studied using Total Current Spectroscopy (TCS). In this technique, a beam of low energy electrons are directed at a sample, and the current through the sample as a function of accelerating voltage is measured. The resultant spectrum provides a great deal of information about the electronic states of the surface[6],[7].

If time permits, the system will be modified to allow for the optical spectrum produced by electron bombardment of a sample to be observed.

1.4 Status

The preparation of thin films of gold and silver nanostructures under different pressures has been investigated. In particular,"gold-black" and "silver-black" films were created using the methods described by Harris[8] and Pfund[9]. Initial measurements of the transmisitivity of "gold-black" films appear to aggree with the results of Harris[10].

Atomic Force Microscopy (AFM) and Scanning Electron Microscopy (SEM) images of gold and silver "black" films on silicon have been taken by the Centre for Microscopy Characterisation and Analysis (CMCA) at UWA. These images provide valuable information about the geometrical structure of "metal-black" films compared to nano-structured films of the same material prepared under high vacuum.

The use of the VASE for the acquisition of both ellipsometric and Reflection and Transmission data has been investigated. Currently, procedures for modelling experimental results from Transmission data of the "black" films are being explored.

2 Benefits

In the last 50 years the world has undergone a revolution in terms of electronic computing. In 1965, Gordon Moore predicted the continued exponential increase in the number of components that could be fit on an integrated circuit, and this law is still famous today[11]. However, at some point it is inevitable that the limit for speed and efficiency of electronic circuits is reached. Research performed for this honours project will explore effects on a nano scale which may be exploited for use in photon/plasmonic based circuitry as an alternative to electronic circuits, allowing further decreases in the size of computing components and increase in the speed of performance.

3 Publications

At CAMSP, Ellipsometry has been used for many years for the characterisation of thin films. In particular, the VASE has been used to investigate the Magneto-Optic Kerr Effect (MOKE) [12],[13]. Electron Spectroscopy, including Electron Energy Loss Spectroscopy (EELS) is also used widely at CAMSP for the characterisation of plasmonic effects.

After the initial description of so called "metal-blacks" by Pfund in the 1930s [9], [14], much research into optical properties was conducted by Harris and others at MIT[8], [10], [15]. This research includes accurate theoretical models for the conductivity and optical constants of "metal-blacks"[15], and experimental data was collected mostly using transmission spectroscopy. Most recently, "gold-black" coatings have been shown to lead to an increase in the efficiency of solar cells, with numerical modelling suggesting that plasmonic effects are responsible[2]. However direct experimental evidence for plasmonic behaviour in metal-black films has not yet been obtained.

Plasmons are electron density oscillations in a solid. The theory of plasmon oscillations was developed in the 1950s by Pines and Bohm[16],[17] to explain electron energy losses in scattering experiments. Recently, the use of Ellipsometry for characterising plasmonic effects has been reviewed by Oates[18].

Komolov [7] and Mller[6] have published extensive works on the setup and use of TCS for characterising surfaces.

4 Costs

Much of the equipment required, including the Ellipsometer, Optical Spectrometer, vacuum chamber (and pumps) and power supplies, is already available at CAMSP. The total estimated cost of the project is $1000. This includes:

- 10 hours workshop time ($40 \times 10 = \$400$)
- Electronic components ($300)
- Deposition materials ($300)

References

[1] Ivan S. Maksymov. Optical switching and logic gates with hybrid plasmonicphotonic crystal, nanobeam cavities. *Physics Letters A*, 2010.

[2] Deep R. Panjwani. Metal blacks as scattering centers to increase the efficiency of thin film solar cells (thesis). *Department of Physics, University of Central Florida*, 2011.

[3] Arthur R. Davoyan Ivan S. Maksymov and Yuri S. Kivshar. Enhanced emission and light control with tapered plasmonic nanoantennas. *Applied Physics Letters*, 2011.

[4] John A. Woolam and Co. Overview of variable angle spectroscopic ellipsometry (vase), part i: Basic theory and typical applications. *Optical Metrology*, 2000.

[5] Harland G. Tompkins. *A User's Guide to Ellipsometry*. Dover Publications, 1992.

[6] M.H. Mohamed P.J. Mller. Total current spectroscopy. *Vacuum*, 35(1):29–37, 1985.

[7] L.T. Chadderton S.A. Komolov. Total current spectroscopy. *Surface Science*, 90(2):359–380, 1979.

[8] Benjamin M. Siegel Louis Harris, Rosemary T. McGinnies. The preparation and optical properties of gold blacks. *Journal of the Optical Society of America*, 1948.

[9] A. H Pfund. Bismuth black and its applications. *Review of Scientific Instruments*, 1930.

[10] Louis Harris and John K. Beasley. The infrared properties of gold smoke deposits. *Journal of the Optical Society of America*, 1952.

[11] Gordon Moore. Cramming more components onto integrated circuits. *Research and Development Laboratories, Fairchild Semiconductor division of Fairchild Camera and Instrument Corp.*, 1965.

[12] Nikita Kostylev. Plasmonic excitations in nanostructures (thesis). *School of Physics, Western Australia*, 2011.

[13] E. Heenan. Spectroscopic ellipsometric characterisation of optical properties of thin films (thesis). *School of Physics, UWA*, 1998.

[14] A. H Pfund. The optical properties of metallic and crystalline powders. *Journal of the Optical Society of America*, 1933.

[15] Louis Harris and Arthur L. Loeb. Conductance and relaxation time of electrons in gold blacks from transmission and reflection measurements in the far infrared. *Journal of the Optical Society of America*, 43(11), 1953.

[16] David Bohm and David Pines. A collective description of electron interactions. i. magnetic interactions. *Phys. Rev.*, 82:625–634, Jun 1951.

[17] David Pines and David Bohm. A collective description of electron interactions: Ii. collective vs individual particle aspects of the interactions. *Phys. Rev.*, 85:338–353, Jan 1952.

[18] H. Arwin T.W.H Oats, H. Wormeester. Characterization of plasmonic effects in thin films and metamaterials using spectroscopic ellipsometry. *Progress in Surface Science (Elsevier Ltd)*, 2011.